Bull. Chem. Soc. Jpn., **72**, 21—26 (1999)

Unusual Electrical Properties of Neutral Mixed-Stack Charge-Transfer Complexes of DAP–BRL (DAP = 1,6-Diaminopyrene, BRL = *p*-Bromanil)

Tasuku Fujinawa, Hirotoshi Goto, Toshio Naito, Tamotsu Inabe,* Tomoyuki Akutagawa,† and Takayoshi Nakamura†

Division of Chemistry, Graduate School of Science, Hokkaido University, Sapporo 060-0810

†Research Institute for Electronic Science, Hokkaido University, Sapporo 060-0812

(Received July 31, 1998)

Two polymorphs of 1 : 1 charge-transfer complexes of DAP–BRL were grown from a benzene solution. The γ-form is triclinic, space group $P\bar{1}$, $a = 16.53(1)$, $b = 17.80(1)$, $c = 8.235(5)$ Å, $\alpha = 96.42(7)$, $\beta = 97.76(6)$, $\gamma = 120.79(5)^\circ$, $V = 2015(3)$ Å^3, and $Z = 4$; the δ-form is monoclinic, space group Pn, $a = 6.862(3)$, $b = 9.891(2)$, $c = 15.246(2)$ Å, $\beta = 101.78(2)^\circ$, $V = 1012.9(5)$ Å^3, and $Z = 2$. Both crystals comprise mixed stacks of donors and acceptors. The molecular geometry, the CO stretching frequencies, and the EPR spectra indicate that most of the component molecules in both crystals are in the neutral state. The electrical conductivity is, however, found to be high; especially the value for γ-DAP–BRL (10^{-1} Ω^{-1} cm^{-1}) is unusually high as a neutral mixed-stack complex.

We recently reported that DAP–CHL (CHL = *p*-chloranil) shows unusual electrical properties.[1] Two polymorphs of this charge-transfer complex, α- and β-DAP–CHL, were obtained from the same benzene solution. Their electrical resistivities of the pristine crystals are ca. 10^8 Ω cm, which is consistent with their crystal structure and electronic state, namely the crystals comprise mixed stacks of neutral donors and acceptors. However, they show an irreversible resistivity change upon heating the sample; the resistivity of the β-form gradually decreases to 10^3 Ω cm at around 400 K, while that of the α-form decreases abruptly to about 10^0 Ω cm at typically around 340 K. Interestingly, neither an X-ray structure analysis nor vibrational and solid-state NMR spectroscopies of low-resistance α-DAP–CHL can detect any change in its crystal structure or the electronic state of the molecules upon this dramatic change in the conductivity. Furthermore, the low-resistance form of α-DAP–CHL can be obtained by simply crushing the crystal into powder. This quite low-resistivity value of α-DAP–CHL is curious, since both the structural and electronic characteristics, "mixed-stacks" of "neutral" donors and acceptors, are quite disadvantageous to electrical conduction. Only by EPR measurements can a small difference between the high- and low-resistance forms be detected; a few % of the ionized species are produced during the resistivity change. This concentration of the ionized species is still insufficient to explain its high conductivity. The difference between the oxidation potential of DAP and the reduction potential of CHL is expected to lead to an ionic complex, since the difference is smaller than that of TTF–CHL, which is situated on the boundary between the ionic and neutral ground states.[2] These facts are considered to be closely related to its unusual electrical properties.

BRL has a similar chemical structure to CHL, and its redox potential is also very close to that of CHL. As a systematic study of DAP complexes, the crystal structures and physical properties of DAP–BRL were thus examined (Chart 1). Similar to DAP–CHL, DAP–BRL has been found to crystallize into two polymorphs from a benzene solution. Originally, the polymorphism of DAP–BRL was noticed by Koizumi and Matsunaga,[3] and two discovered polymorphs were assumed to be similar to DAP–CHL. We found that they are distinguishable from the polymorphs of DAP–CHL, and are here called as γ- and δ-DAP–BRL. In this paper we describe their crystal structures and electrical properties, especially for γ-DAP–BRL, which shows high conductivity despite its neutral mixed-stack structure.

Experimental

Materials. DAP was synthesized[4] and purified by a reported method.[1] BRL was commercially purchased and purified by recrystallization followed by vacuum sublimation. Single crystals of DAP–BRL were grown by slow cooling and prolonged slow evaporation of a benzene solution. Two polymorphs of DAP–BRL were simultaneously obtained from the benzene solution.

Measurements. Electrical-conductivity measurements were carried out using a four-probe method for low-resistance samples and a two-probe method for high-resistance samples. The infrared

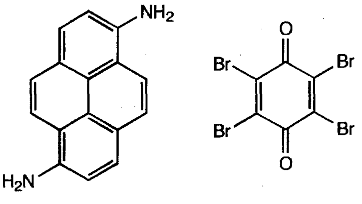

Chart 1.

spectra were recorded on a Perkin–Elmer 1650 FT-IR spectrometer. EPR measurements were performed using a JEOL JES-FE1X spectrometer.

X-Ray Structure Analysis. A single crystal of δ-DAP–BRL with dimensions of $0.48\times0.40\times0.15$ mm^3 was used for an X-ray structure analysis. An automated Rigaku AFC-5R diffractometer with graphite-monochromatized Mo $K\alpha$ radiation (λ = 0.71073 Å) was used for data collection at 296 K. The data were corrected for Lorentz and polarization effects, and an absorption correction was also applied. Three standard reflections monitored every 150 data measurements showed no significant deviation in the intensities. The data-collection conditions and crystal data are summarized in Table 1. The crystal structure of δ-DAP–BRLwas solved by the Patterson method. The positions of all the hydrogen atoms were determined from a difference synthesis map, and a block-diagonal least-squares technique (UNICS III[5]) with anisotropic thermal parameters for non-hydrogen atoms and isotropic for hydrogen atoms was employed for a structure refinement.

X-Ray diffraction experiments of γ-DAP–BRL were performed with a small single-crystal ($0.2\times0.1\times0.03$ mm^3). Consequently, the structure analysis is not complete, and the data are preliminary.[6]

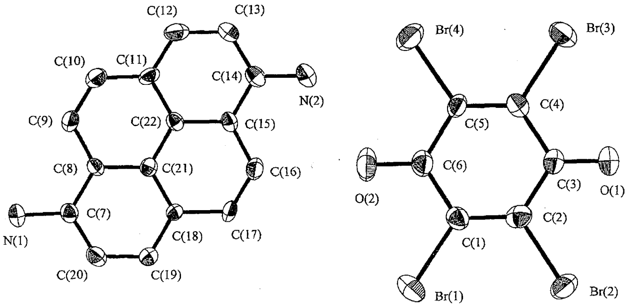

Fig. 1. ORTEP drawing of DAP and BRL in δ-DAP–BRL showing the atom numbering scheme.

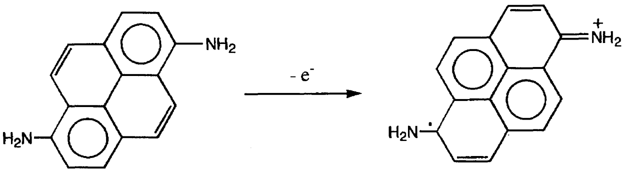

Scheme 1.

Results

Crystal Structure of δ-DAP–BRL. The molecular structure derived from an X-ray structure analysis of δ-DAP–BRL is shown in Fig. 1, and the atomic parameters are given in Table 2.[7] The bond lengths are sometimes a good index of the oxidation state. Unfortunately, there are not sufficient data for BRL. On the other hand, the bond-length data for DAP are available for the neutral and cation radical states. These data are listed together with the data for δ-DAP–BRL in Table 3. The aromatic ring in DAP is localized at two terminal aniline rings in the neutral state, while it is moved to the central naphthalene ring upon removing one electron from the π-system as shown in Scheme 1. The bond alternation of *i-j-k* is clear in neutral DAP, while it is much less in DAP$^+$. On the other hand, a bond alternation of *a-g-f-e* can be seen in DAP$^+$, while it is not significant in neutral DAP. By comparing the data for δ-DAP–BRL with them, DAP in δ-DAP–BRL can be regarded as neutral. Another method for evaluating the degree of ionization is the frequency of the CO stretching mode in the infrared spectrum. The frequency is 1677 cm^{-1} for neutral BRL, while it is reported to be shifted

Table 1. Data-Collection Conditions and Crystal Data

	γ-DAP–BRL	δ-DAP–BRL
Chemical formula	$C_{22}H_{12}Br_4N_2O_2$	$C_{22}H_{12}Br_4N_2O_2$
Molecular weight	655.97	655.97
Crystal system	Triclinic	Monoclinic
Space group	$P\overline{1}$	Pn
a/Å	16.53(1)	6.862(3)
b/Å	17.80(1)	9.891(2)
c/Å	8.235(5)	15.246(2)
α/deg	96.42(7)	90.00
β/deg	97.76(6)	101.78(2)
γ/deg	120.79(5)	90.00
V/Å^3	2015(3)	1012.9(5)
Z	4	2
D_{calcd}/g cm^{-3}	2.161	2.151
μ(Mo $K\alpha$)/cm^{-1}	80.34	78.94
2θ range	$5^\circ < 2\theta < 60^\circ$	$5^\circ < 2\theta < 60^\circ$
Scan width/deg	$1.2 + 0.5\tan\theta$	$1.1 + 0.3\tan\theta$
Scan mode	ω–2θ	ω–2θ
Scan rate/deg min^{-1}	5	4
Number of reflections measured	8183	3349
Number of independent reflections observed	1518 ($I_o > 4\sigma(I_o)$)	2457 ($F_o > 3\sigma(F_o)$)
Number of parameters	281	320
R	0.097	0.036
R_w	0.122	0.035

Table 2. Fractional Coordinates and Equivalent Temperature Factors for δ-DAP–BRL

Atom	x	y	z	$B_{eq}/Å^2$
Br(1)	0.0106(1)	0.3998(1)	0.0044(1)	3.1(1)
Br(2)	0.4338(1)	0.5627(1)	−0.0122(1)	3.6(1)
Br(3)	0.4127(1)	0.8486(1)	0.3070(1)	3.5(1)
Br(4)	−0.0180(1)	0.6907(1)	0.3206(1)	3.8(1)
O(1)	0.5317(7)	0.7658(5)	0.1360(3)	3.5(1)
O(2)	−0.1302(7)	0.5007(5)	0.1643(3)	3.8(1)
C(1)	0.1280(9)	0.5333(6)	0.0855(4)	2.4(1)
C(2)	0.2985(9)	0.5988(6)	0.0803(4)	2.6(1)
C(3)	0.3867(9)	0.7014(6)	0.1445(4)	2.5(1)
C(4)	0.2858(8)	0.7257(6)	0.2209(4)	2.4(1)
C(5)	0.1156(8)	0.6636(6)	0.2270(4)	2.2(1)
C(6)	0.0230(9)	0.5612(6)	0.1588(4)	2.6(1)
N(1)	0.5496(8)	0.4641(5)	0.2620(4)	3.3(1)
N(2)	−0.1384(9)	−0.2144(6)	0.0221(4)	3.8(2)
C(7)	0.4026(8)	0.3652(6)	0.2528(4)	2.2(1)
C(8)	0.3825(8)	0.2645(5)	0.1842(3)	1.9(1)
C(9)	0.5124(9)	0.2556(6)	0.1233(4)	2.6(1)
C(10)	0.4851(10)	0.1620(6)	0.0575(4)	2.9(2)
C(11)	0.3253(9)	0.0682(6)	0.0451(4)	2.6(1)
C(12)	0.2917(10)	−0.0276(6)	−0.0227(4)	3.2(2)
C(13)	0.1349(10)	−0.1183(6)	−0.0316(5)	3.2(2)
C(14)	0.0062(9)	−0.1189(6)	0.0287(4)	2.7(2)
C(15)	0.0355(8)	−0.0223(5)	0.0987(4)	2.1(1)
C(16)	−0.0944(9)	−0.0152(6)	0.1620(4)	2.8(1)
C(17)	−0.0688(9)	0.0782(6)	0.2266(4)	2.7(2)
C(18)	0.0922(8)	0.1768(5)	0.2362(4)	2.0(1)
C(19)	0.1129(9)	0.2768(6)	0.3019(4)	2.6(1)
C(20)	0.2673(9)	0.3695(6)	0.3095(4)	2.6(1)
C(21)	0.2244(8)	0.1700(5)	0.1764(4)	2.0(1)
C(22)	0.1982(8)	0.0720(5)	0.1074(4)	2.0(1)

Table 3. Bond Lengths of DAP

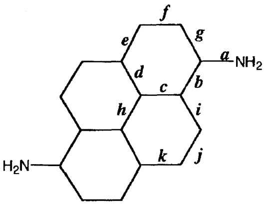

Bond	DAP^0 (α-DAP–CHL[a])	DAP^+ (DAP–TCNQ[b])	δ-DAP–BRL
a	1.387(2)	1.334(2)	1.375(16)
b	1.415(2)	1.440(1)	1.423(8)
c	1.424(2)	1.424(2)	1.429(11)
d	1.425(2)	1.422(1)	1.414(9)
e	1.398(2)	1.428(1)	1.391(9)
f	1.377(3)	1.360(2)	1.387(9)
g	1.396(3)	1.427(2)	1.396(10)
h	1.435(1)	1.424(1)	1.415(8)
i	1.436(3)	1.408(2)	1.430(14)
j	1.352(2)	1.371(1)	1.343(9)
k	1.431(2)	1.413(2)	1.439(19)

a) Ref. 1. b) Ref. 9.

to 1518 cm^{-1} for K^+BRL^-.[8] The value for δ-DAP–BRL is 1652 cm^{-1}, and the charge on BRL is estimated to be −0.16 by assuming that the shift is linearly correlated to the charge.

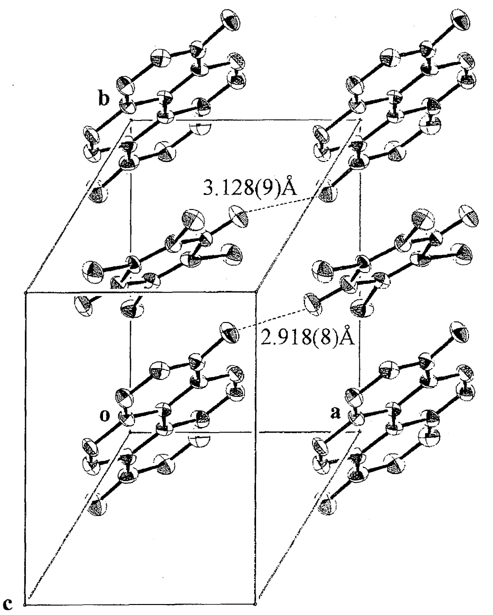

Fig. 2. Crystal structure of δ-DAP–BRL.

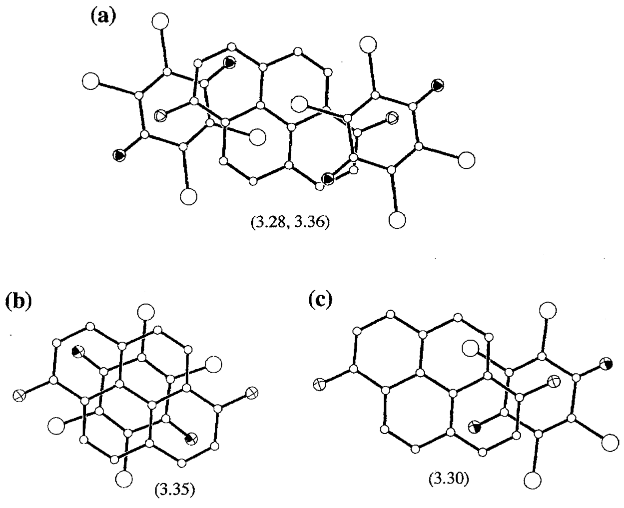

Fig. 3. Molecular overlap in δ-DAP–BRL (**a**), α-DAP–CHL (**b**), and β-DAP–CHL (**c**). Numbers in parentheses are the interplanar distance (Å).

The estimated value seems to be somewhat larger than that expected from the bond lengths of DAP. Similarly, the EPR measurements suggest a much smaller value of the degree of ionization (vide infra).

The crystal structure of δ-DAP–BRL is shown in Fig. 2. The DAP and BRL molecules are alternately stacked along the b-axis. There are two kinds of N–H···O hydrogen bonds between these one-dimensional columns: 2.918(8) and 3.128(9) Å. The molecular overlap is shown in Fig. 3. As can be seen from Fig. 3, the overlapping mode is similar to that in β-DAP–CHL. In addition, donors and acceptors are not parallel in both structures; the dihedral angle is ca. 7.3° in both cases. The difference lies in the symmetry; molecules are at general positions in δ-DAP–BRL, while they are located on the inversion centers in β-DAP–CHL.

Crystal Structure of γ-DAP–BRL. Although crystal growth was attempted under various conditions, it was extremely difficult to obtain a crystal with sufficient size and quality. This may have been because γ-DAP–BRL is a metastable phase. At the initial stage of crystal growth, nucleation of γ-DAP–BRL occurs preferentially. However, the growth always stops at some stage, and thermodynamically more stable δ-DAP–BRL begins to grow. Thus, we cannot perform X-ray diffraction experiments using a large high-quality single crystal. The crystal data in Table 1 were obtained using the best single crystal obtained so far. Using these parameters, the powder-diffraction pattern of γ-DAP–BRL was satisfactorily indexed. The crystal structure is shown in Fig. 4. In the unit cell, there are four donor–acceptor pairs, and all of the component molecules are located on the inversion centers. Consequently, there are four kinds of one-dimensional columns along the *c*-axis, each of which comprises mixed stacks of donors and acceptors. As can be seen from Fig. 4, three of them (columns I, II, and III) are bound to each other by hydrogen bonds, forming a network in the crystal. Column IV occupies a one-dimensional space surrounded by a pair of columns I, II, and III, and does not form hydrogen bonds with other columns. The thermal parameters of the molecules, especially DAP, in column IV are unusually large, suggesting the existence of a positional disorder. The degree of disorder is not so large that the donor-site and acceptor-site are indistinguishable, since no large electron density due to Br can be detected at the donor-site; namely, the mixed-stacking order is still retained. Another possibility of large thermal parameters for the molecules in column IV could be smaller site occupation. Although refinements with smaller site occupancies were tried, there was no improvement in the thermal parameters and the *R* value. In addition, density measurements indicate only a small deference from the calculated value for a perfect crystal ($d_{\mathrm{obs}} = 2.15\ \mathrm{g\,cm^{-3}}$ vs. $d_{\mathrm{calc}} = 2.161\ \mathrm{g\,cm^{-3}}$). Although the refinement was so imperfect that we cannot discuss any details of the structure, it is safe to say that the crystal comprises mixed stacks of donors and acceptors.

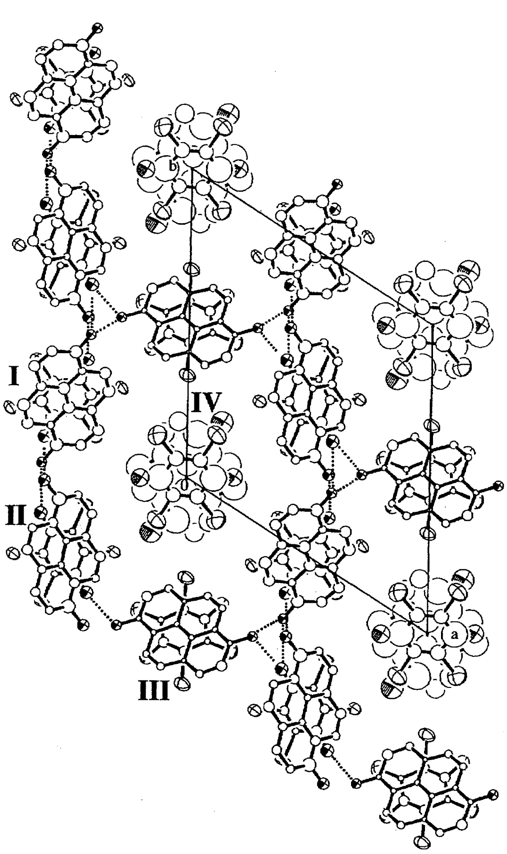

Fig. 4. Crystal structure of γ-DAP–BRL. Broken lines indicate hydrogen bonds (including the bond with molecule at $z\pm1$).

An attempt was made to estimate the ground state of γ-DAP–BRL from the infrared data. The CO stretching mode was observed at 1665 $\mathrm{cm^{-1}}$, and the degree of ionization was estimated to be 0.08. Again, the ground state of this crystal is suggested to be close to the neutral one.

Electrical Conductivity. The electrical conductivities of γ- and δ-DAP–BRL are expected to be low, since both crystals comprise mixed stacks of neutral donors and acceptors. Their electrical resistivities are shown in Fig. 5. Contrary to the general expectation, they are rather conductive. Especially, the resistivity at room temperature for γ-DAP–BRL (ca. 10 Ω cm) is unusually low as a neutral mixed-stack complex. This value is comparable to that of low-resistance α-DAP–CHL. In contrast to α-DAP–CHL, γ-DAP–BRL is already in the low-resistance state during the initial stage, and no further resistivity drop is observed when the temperature increases. On the other hand, the δ-form shows small and gradual drop of resistivity. This change is irreversible, as observed for DAP–CHL, and the resistivity at room temperature is nearly the same as that of the low-resistance state of β-DAP–CHL.

Magnetic Susceptibility Obtained from EPR Spectra. Figure 6 shows the paramagnetic susceptibility (χ_{p}) of γ- and low-resistance δ-DAP–BRL evaluated from the EPR signal intensity. The behavior of γ-DAP–BRL, in which χ_{p} decreases with decreasing temperature, is again similar to

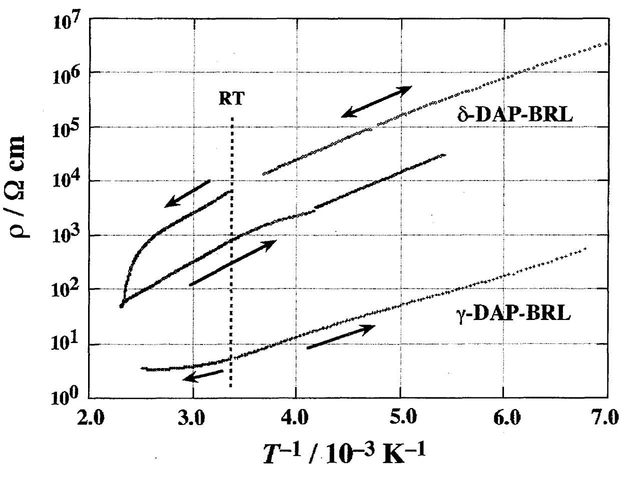

Fig. 5. Temperature dependence of the electrical resistivity of γ-DAP–BRL and δ-DAP–BRL. Arrows indicate the direction of the temperature change.

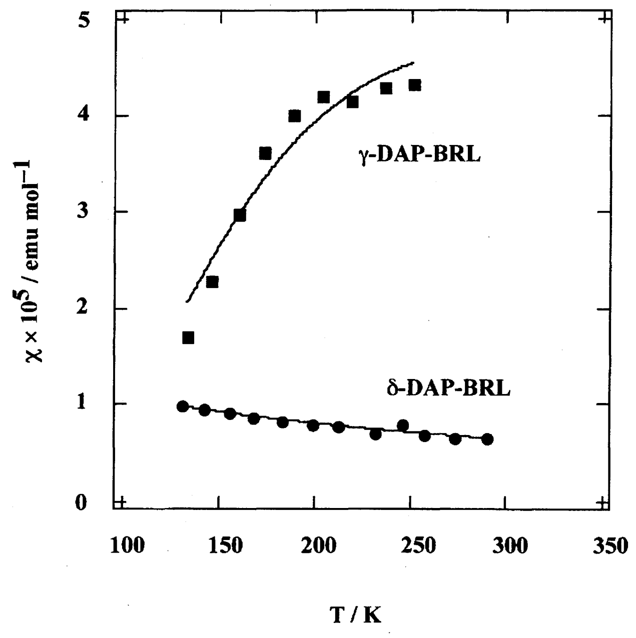

Fig. 6. Paramagnetic susceptibility of DAP–BRL evaluated from the ESR signal intensity. Lines are fitting using the singlet–triplet type for γ-DAP–BRL and the Curie–Weiss type for δ-DAP–BRL.

that of low-resistance α-DAP–CHL. With assuming the thermally activated paramagnetism as excitation from the singlet- to triplet-state, the concentration of the ionized species in γ-DAP–BRL is estimated to be ca. 4% of the donor–acceptor pairs. Interestingly, the temperature dependence of low-resistance δ-DAP–BRL shows the opposite behavior, in which χ_p increases with decreasing temperature. This behavior corresponds well to that of low-resistance β-DAP–CHL. Upon assuming the Curie–Weiss law, concentration of the ionized species in δ-DAP–BRL is estimated to be ca. 0.5% of the donor–acceptor pairs (Weiss temperature = -185 K). The concentrations of ionized species in γ- and δ-DAP–BRL are smaller than those estimated from the CO stretching frequencies. Since the molecular geometry determined from an X-ray structure analysis of δ-DAP–BRL strongly suggests that the molecule is quite close to the neutral state, the concentration values estimated from a sensitive EPR method may be more reliable than those estimated from the IR spectra.

Discussion

The main features observed for DAP–BRL are quite similar to those observed for DAP–CHL. The crystals comprise mixed stacks of neutral donors and acceptors. The resistivity of δ-DAP–BRL may be interpreted by a small amount of ionized species, since the value is in the range of impurity semiconductors. The resistivity value of γ-DAP–BRL (10 Ω cm) is unusually low, and corresponds to that of low-resistance α-DAP–CHL. Both γ-DAP–BRL and low-resistance α-DAP–CHL show a singlet-triplet-like thermally activated paramagnetic susceptibility in common, showing that spins of ionized species are paired in the ground state, even for quite low concentrations. If the spins (electrons) released from the singlet state by thermal excitation are assumed to be able to travel in the crystal, current flow becomes possible. In this case, the energy of excitation from the singlet ground state must be smaller than the activation energy of conduction, since the activation energy of conduction involves not only the carrier-generation process, but also the transport process (hopping of carriers). The singlet-to-triplet excitation energy is estimated to be ca. 500 K (0.04 eV) for low-resistance α-DAP–CHL and ca. 250 K (0.02 eV) for γ-DAP–BRL based on the temperature dependence of the magnetic susceptibility. The activation energies of conduction are 0.08—0.15 eV for low-resistance α-DAP–CHL and 0.10 eV for γ-DAP–BRL. These values are not inconsistent with the above assumption. Such a situation occurring in a one-dimensional column is schematically shown in Fig. 7(a). In this case, a pair of thermally excited spins need to move to opposite directions from each other for current flow. For this process, excitation of $\text{D–A} \rightarrow \text{D}^+\text{–A}^-$ of the next pairs should always be associated. Since the complexes do not take an ionic ground state, this energy must be larger than the Coulombic attraction energy, which is expected to be gained when they take an ionic ground state. The Coulombic attraction energy can be evaluated from the D–A distance; as an example, it amounts 3.5 eV for γ-DAP–BRL. Even if this value is greatly reduced by other factors, it is still extremely larger than the energy scale considered here. Consequently, high conductivity cannot be achieved.

Another noticeable feature of this system is the intermolecular hydrogen bonds. By this interaction, one-dimensional columns are bound to each other and form a two-dimensional sheet (α-DAP–CHL) or three-dimensional network (γ-DAP–BRL). The possibility of an electronic interaction between the columns is suggested from their conduction anisotropy. The anisotropy is always small; the value for $\rho_{\perp}/\rho_{//}$ is < 10 for low-resistance α-DAP–CHL and ca. 10 for γ-DAP–BRL. If this interaction can play a role to make a spin pair as shown in Fig. 7(b), the situation might be modified. In this case, the thermal excitation will result in the doping of an ionized species in a mixed-stacked col-

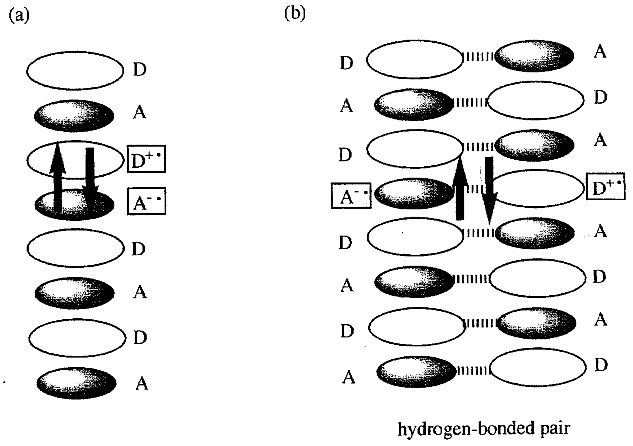

Fig. 7. Schematic representation of the singlet pair in the DAP complexes. A pair in the one-dimensional column (a) and a pair formed by the hydrogen bond (b).

umn. This situation is completely different from the above situation in which the ionized pair is doped. The question whether such a doping can lead to a highly conducting state or not is a completely unsolved problem.

There is another question about the ground states of DAP–CHL and DAP–BRL. The difference between the redox potentials is so small that the ground state can be ionic. If the transfer energy between the donor and acceptor is extremely small, namely there is no virtual overlap between HOMO of the donor and LUMO of the acceptor, an electron cannot transfer, and a neutral ground state could be achieved. Preliminary calculations of the overlap integral between DAP and acceptors in each column have been made by an extended Hückel method. Although the value for α-DAP–CHL seems to be small, for the others the overlap integral values are nearly 10^{-2}. This value is not unusually small compared with other charge-transfer complexes, and at the present stage no rationalized explanation for their neutral ground state can be given. An attempt to combine DAP with stronger acceptors to obtain ionic mixed-stack DAP complexes as well as a systematic evaluation of the overlap integrals are now in progress.

In conclusion, we have found that one of the two polymorphs of DAP–BRL, γ-DAP–BRL, shows high conductivity. This is rather unusual, since the crystal comprises mixed stacks of neutral donors and acceptors. A small amount of ionized species, of which the magnetism is a thermally activated type, detected by an EPR measurement, is a common peculiarity for highly conducting mixed-stack DAP complexes.

This work was partly supported by a Grant-in-Aid for Scientific Research No. 07454181 from the Ministry of Education, Science, Sports and Culture.

References

1) H. Goto, T. Fujinawa, H. Asahi, T. Inabe, H. Ogata, S. Miyajima, and Y. Maruyama, *Bull. Chem. Soc. Jpn.*, **69**, 85 (1996).

2) J. B. Torrance, J. E. Vazquez, J. J. Mayerle, and V. Y. Lee, *Phys. Rev. Lett.*, **46**, 253 (1981).

3) S. Koizumi and Y. Matsunaga, *Bull. Chem. Soc. Jpn.*, **45**, 432 (1972).

4) H. Vollman, H. Becker, M. Corell, H. Streek, and G. Langbein, *Justus Liebigs Ann. Chem.*, **531**, 1 (1937).

5) T. Sakurai and K. Kobayashi, *Rep. Inst. Phys. Chem. Res.*, **55**, 69 (1979).

6) The anisotropic thermal parameters were applied only for bromine atoms, and the other atoms were treated as isotropic.

7) The lists of structure factors and anisotropic thermal parameters for non-hydrogen atoms are deposited as Document No. 71070 at the Office of the Editor of Bull. Chem. Soc. Jpn.

8) A. Girlando, I. Zanon, R. Bozio, and C. Pecile, *J. Chem. Phys.*, **68**, 22 (1978).

9) T. Inabe, K. Okaniwa, H. Ogata, H. Okamoto, T. Mitani, and Y. Maruyama, *Acta Chim. Hungarica–Models in Chem.*, **130**, 537 (1993).